ISBN: 978-3-95450-231-8 ISSN: 2673-5490 doi: 10.18429/JACoW-IPAC2023-THPL172

BEAD-PULL ANALYSIS OF HOM IN X-BAND LINEARIZER LINAC ON CLARA, WITH UPDATE ON HOM MEASUREMENT SYSTEM *

N. Y. Joshi†[1], A. Farricker[1], A. Gilfellon[1], C. Jenkins[1], A. Moss[1]
ASTeC, STFC Daresbury Laboratory, Sci-Tech Daresbury, Warrington, UK
[1]also at The Cockcroft Institute, Sci-Tech Daresbury, Warrington, UK
B. T. Green, Lancaster University, Engineering dept, Bailrigg, UK
M. Elfleet, University of Glasgow, School of Engineering, Glasgow, UK

Abstract

The X-band lineariser linac planned to be installed on CLARA will be aligned using beam induced higher order modes (HOMs). Higher order modes in the cavity were studied using a bead-pull measurement technique. A software application was developed in LabVIEW to control the 3D motorised bead position scanning setup and VNA for S-parameter measurements. Propagation of HOM frequencies in the linac were verified, identifying the most suitable HOMs to use. Progress in development of HOM signal processing hardware system with dynamic control is also discussed in the paper.

INTRODUCTION

CLARA is being developed in phases to serve as a test platform for new concepts and technologies for future large scale XFEL facilities. With additional 2.9985 GHz normal conducting RF accelerating structures installed as part of the upgrade to phase-II, it will bring the nominal electron beam energy up to 250 MeV [1, 2]. It will also utilise a fourth harmonic X-band linac to linearise the bunch longitudinal phase space. The X-band linac will be installed on a five axis precision mover. The linac was designed by PSI in collaboration with CERN. The relevant parameters of the X-band linac are summarised in Table 1 [3–5].

Table 1: Relevant Specifications of the X-band Linac Cavity

Parameter	Value	Unit
Fundamental frequency	11.994	GHz
Effective Length	75	cm
Number of cells	72	
Phase advance	$5\pi/6$	
HOM coupling cells	2	
HOM frequency range	15.3 - 16.2	GHz
HOM impedance	~ 100	$k\Omega/(mm \times m)$

An electron bunch passing through the linac induces an electromagnetic (EM) field, known as wakefield, which can be expressed as a sum of the field induced in the fundamental and various HOMs. The induced HOM field interacts back with the bunch and degrades beam quality, hence it is desirable to minimise HOM excitation in the linac. The amplitude of the induced dipole HOMs depends on the bunch charge and transverse bunch offset from the cylindrical axis of the linac [4]. The phase of the HOM field flips by 180 ° depending on the direction of offset from the centre. By coupling out and analysing the HOM field signals, bunch trajectory offset and angle can be determined and used to minimise HOM excitation. The linac cell iris and radius are varied along the linac length to achieve the desired gradient profile of the fundamental accelerating field, which also results in variation of the dipole HOM frequencies of the cells.

The X band linac has two HOM couplers, the first is located in the mid section of the linac and couples to the HOMs from upstream cells. The second is at the end of the linac and couples to the HOMs from the downstream cells situated after the first HOM coupler. The HOMs are coupled out through the side coupled waveguides with cutoff frequency above the fundamental accelerating frequency to prevent the large accelerating field at 11.994 GHz. Each HOM cell has four ports, two each for X and Y bunch offset measurements, which can be combined to increase measurement sensitivity. HOMs generated in different cavity cells propagate with different time delays resulting in a net output signal that can be complex and difficult to measure and analyse for cavity alignment. To overcome this challenge, the wakefield monitor system [6] will use a direct digital synthesis (DDS) based local oscillator (LO) with frequency tuning to select individual HOM for measurement. For better alignment of the cavity HOMs that are excited towards either upstream or downstream end of the linac, with good propagation through cavity and coupling the HOM port should be used for the measurement.

Propagation of different HOM frequencies along the linac and coupling efficient to HOM port have been studied using a bead-pull measurement setup. Theory and working principle of bead-pull method are well documented [7, 8], which usually includes insertion of a small spherical dielectric bead into the resonant cavity structure, changing the effective dielectric constant locally within the cell. Within the small perturbation regime, the shift in resonance frequency peak and phase at the resonance frequency can be related to a non-magnetic dielectric bead as [9, 10],

$$\frac{tan\phi(f_0)}{2Q} = \frac{\Delta f}{f_0} = -\frac{\pi r^3}{U}[\epsilon_0 \frac{\epsilon_r - 1}{\epsilon_r + 2} E_0^2], \qquad (1)$$

* STFC-UKRI
† Nirav.Joshi@stfc.ac.uk

ISBN: 978-3-95450-231-8 ISSN: 2673-5490 doi: 10.18429/JACoW-IPAC2023-THPL172

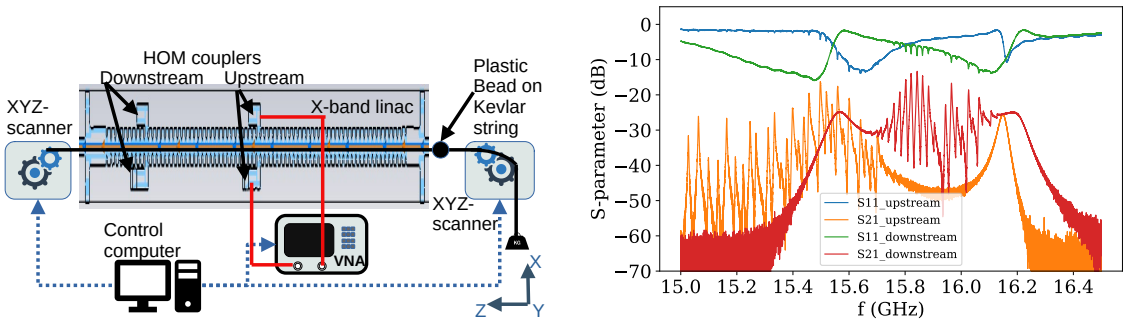

(a) Bead-pull setup, (b) S-parameters,

Figure 1: Block diagram of bead-pull experiment setup, and S-parameters measured at up and downstream HOM couplers.

where, f_0 and Q are the resonance frequency and quality factor of the mode, r and ϵ_r are the radius and relative permittivity of the bead, E_0 and U are the amplitude of the electric field at the bead position and total energy stored inside the cavity respectively. As the cavity has been received from another facility, the design frequency is slightly off from the desired frequency of 11.994 GHz. The cavity is first tuned to the desired fundamental acceleration frequency by optimising its operation temperature while measuring power coupling and field inside the cells at acceleration frequency using the bead-pull technique. After tuning the temperature using the fundamental mode, bead-pull measurement over HOM spectrum was carried out, which is presented in this paper.

S-PARAMETER AND BEAD-PULL MEASUREMENTS

A block diagram of the bead-pull setup used to measure field pattern at fundamental and HOM frequencies is shown in Fig. 1a. It's a horizontal perturbation rig, with precision motorised position scanners at each end which can set transverse (X and Y axes) position independently of each other, allowing measurement along bead trajectory at different angles compared to the cavity axis. A small plastic bead was attached to a Kevlar thread which is passed through the linac. Kevlar thread was chosen for its tensile strength to minimise drooping of the bead and thread due to gravity. The thread was passed through pulleys on the transverse scanners. One end of the thread was attached to a Z-axis (longitudinal) scanner, while appropriate weight was hung at the other end of the thread to keep it stretched under tension. The transverse scanner has a spacial resolution of 100 μm and scan range of more than 100 mm. Longitudinal Z-axis scanner a has range of more than 1 m. In this mode of bead-pull setup, the Z-position is affected when the transverse position is changed and should be corrected appropriately.

S-parameters were recorded using a two port Vector Network Analyser (VNA), Agilent PNA-N5230C. The opposite HOM ports along X-axis were connected to the VNA to measure reflection and transmission characteristics while the other two HOM ports (along Y-axis) were terminated to match loads. HOM spectrum over 1.5 GHz was measured with a frequency step size of 50 kHz. HOM spectrum at upstream and downstream couplers were measured separately. Reflection and transmission S-parameters measured without a bead are plotted in Fig. 1b. It verified that the upstream HOM spectrum spans from 15.2 to 15.5 GHz, while the downstream HOM spectrum falls between 15.7 to 16.1 GHz. Both of the spectrums are well within the frequency range of the wakefield monitor system under development which can analyse signals between 15.1 to 16.5 GHz.

To carry out bead-pull measurements, a control sequence program was developed in LabVIEW [11] to synchronise bead position scanners and VNA data capture. A LabVIEW program was designed to provide a complete set of functionalities required for initial bead orientation and retaining VNA calibration. Initially the thread was aligned to the cavity axis by manually aligning it to the beam pipe centers at both ends and the bead was then brought to the cavity entrance, which then acted as a origin of the measurement coordinate system. After setting frequency range and maximising RF power for better signal to noise ratio, calibration was applied to remove contributions from the cables and connectors in the setup. The bead trajectory was offset by 1 mm along both X and Y axis in the transverse plane. Bead position was then scanned along the longitudinal Z-axis in step size of 0.5 mm and all reflection and transmission S-parameters were recorded at each position. Complete set of scans for the upstream and downstream couplers each took couple of hours over which the cavity temperature was maintained at the value optimised using monopole measurements.

The phase change caused over the whole recorded HOM spectrum for different bead positions are plotted in Fig. 2a and 2b for upstream and downstream couplers respectively. These bead-pull measurements alone can only confirm propagation and coupling of various HOM frequencies along the linac length. For complete understanding it should be compared with stretch wire measurements of HOMs and simulation of synchronous frequencies. For effective alignment of the linac to beam, any mode that is excited towards one of ends of the linac and has good coupling with HOM port is the most suitable for the measurement. As shown in Fig. 2a, the resonant HOMs around 15.32 and 15.45 GHz

ISBN: 978-3-95450-231-8 ISSN: 2673-5490 doi: 10.18429/JACoW-IPAC2023-THPL172

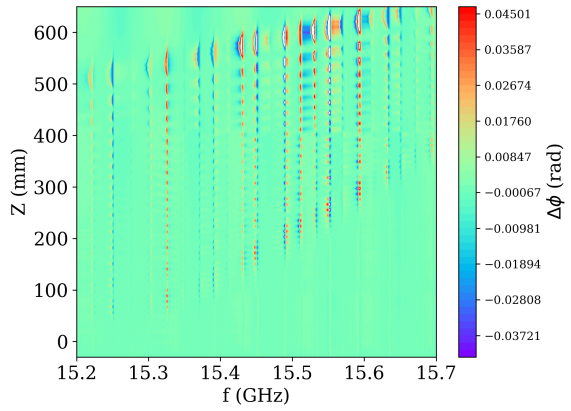

(a) Upstream coupler,

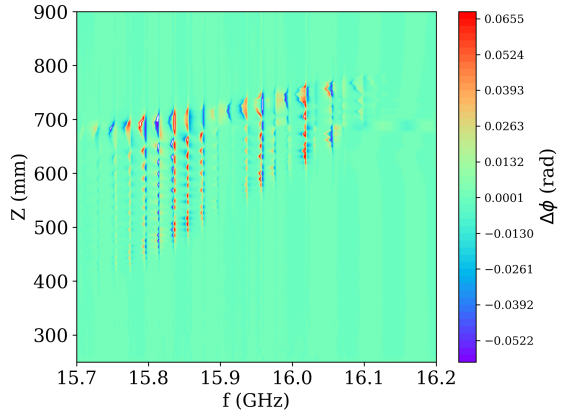

(b) Downstream coupler,

Figure 2: Phase variation at HOM frequencies due to field perturbation caused by bead traversing through the linac.

are propagating through up to the beginning of the linac and have good coupling to the upstream HOM couplers. The downstream coupler benefits from proximity to the end of the cavity and has good coupling with modes towards the end of the linac.

Digital Controls

To facilitate large measurement dynamic range, the frontend box will have in total four pairs of digitally controlled attenuators and switches. The attenuators and switches are controlled using Red Pitaya boards which provides GPIO pins for digital control and also have fast digitisers to measure the RF power and implement onboard control sequence to optimise attenuation level. An EPICS-IOC [12] has been developed based on epics driver support for Red Pitaya [13], to control two frontend channels using one Red Pitaya.

The back-end box utilises DDS based LO boards to facilitate detailed HOM and angular offset analysis by selecting individual mode of interest from the whole HOM spectrum. Four DDS-LO boards are controlled using a Raspberry Pi. An EPICS IOC is developed to implement serial peripheral

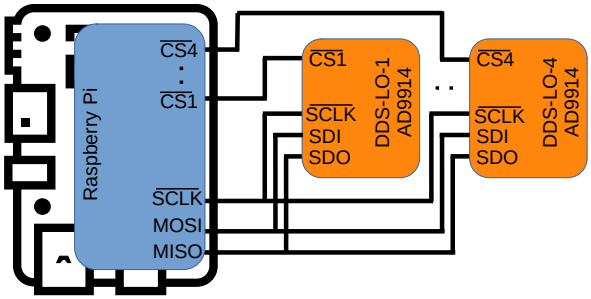

Figure 3: Block diagram of setup to control four DDS-LO boards with one Raspberry Pi using SPI interface.

interface (SPI) protocol to control all four boards, based on previous work [14] utilising epics-devgpio and drvAsynSPI libraries. A simplified block diagram of the control setup is shown in Fig. 3. While using SPI, all four DDS boards share the input and output channels (MOSI and MISO), but only one board at a time is selected using a chip select (CS) pin that will accept the data transfer. Raspberry Pi also provides the synchronous clock (SCLK), and additional functionalities such as board reset and IO-update are also incorporated. EPICS procedures are implemented to initialise the DDS boards and map LO frequency PVs for read and write functions.

SUMMARY

Higher order modes spectrum of the X-band lineariser linac was studied using bead-pull measurements. S-parameter measurements at upstream and downstream HOM couplers verified that HOM spectrums are within the frequency range of 15.1 to 16.5 GHz planned for the wakefield monitor system. A control program was developed in LabVIEW to align the bead trajectory and coordinate RF measurements with position scans allowing automated long measurement runs. Bead-pull analysis identified HOMs propagating effectively through the linac and coupling well to the HOM couplers, which should be most suitable to use with the wakefield monitor system to align the cavity. EPICS IOCs were developed for digital control of the attenuators, switches and LO frequencies using Red Pitaya and Raspberry Pi based digital controllers.

REFERENCES

[1] J. A. Clarke *et al.*, "CLARA Conceptual Design Report", STFC, July. 2013, https://www.ukri.org/publications/clara-conceptual-design-report/

[2] D. Angal-Kalinin *et al.*, "Design, specifications, and first beam measurements of the compact linear accelerator for research and applications front end", *Phys. Rev. Accel. Beams*, vol. 23, no. 4, p. 044801, Apr. 2020. doi:10.1103/PhysRevAccelBeams.23.044801

[3] D. Gudkov *et al.*, "Engineering Design of a Multipurpose X-Band Accelerating Structure", in *Proc. IPAC'10*, Kyoto, Japan, May. 2010. THPEA04207, pp. 3771-3773.

ISBN: 978-3-95450-231-8 ISSN: 2673-5490 doi: 10.18429/JACoW-IPAC2023-THPL172

[4] M. Dehler, A. Citterio, A. Falone, J. Raguin, "X-band rf structure with integrated alignment monitors", *Phys. Rev. Accel. Beams*, vol. 12, p. 062001, June, 2009.

[5] L. S. Cowie *et al.*, "An X-Band Lineariser for the CLARA FEL", in *Proc. IPAC'18*, Vancouver, Canada, Apr.-May 2018, pp. 3848–3851. doi:10.18429/JACoW-IPAC2018-THPAL084

[6] N. Y. Joshi, A. C. Aiken, C. R. Jenkins, and A. J. Moss, "Wakefield Monitor System for X-Band Lineariser Linac on CLARA", in *Proc. LINAC'22*, Liverpool, UK, Aug.-Sep. 2022, pp. 718–720. doi:10.18429/JACoW-LINAC2022-THPOJO11

[7] J. Shi et al., "Tuning of X-band traveling-wave accelerating structures", *Nucl. Instrum. Methods*, A, 704, 2013, p. 14-18.

[8] C. W. Steele, "A Nonresonant Perturbation Theory", *IEEE Trans. Microwave Theory Tech.*, vol. MTT-14, no. 2, 1966, p. 70-74.

[9] P. A. McIntosh, "Perturbation measurement on RF cavities at Daresbury", *Proc. EPAC94*, London, June 1994, p. 1283.

[10] J. Byrd et. al. "Microwave Measurements Laboratory for Accelerators Lecture Material", *USPAS 2013*, Colorado State University, Fort Collins, June 2013.

[11] LabVIEW by National Instrument, https://www.ni.com/en-gb/shop/labview.html

[12] EPICS collaboration team, https://epics.anl.gov

[13] A. Pozar, EPICS driver support for RedPitaya based on asynPortDriver, https://github.com/AustralianSynchrotron/redpitaya-epics

[14] K. Shiro, U. Shinji, and E. Yoshinori, "Development of control software for EPICS compatible DC magnet power supply using Raspberry Pi", *Proc. of the 18th annual meeting of Particle Accelerator Society of Japan*, Japan, 2021, p. 998